

# Delineation of the Dimensions and Permeability Characteristics of the Two Major Diffusion Barriers to Passive Mucosal Uptake in the Rabbit Intestine

HENRIK WESTERGAARD and JOHN M. DIETSCHY

*From the Gastrointestinal-Liver Section of the Department of Medicine, The University of Texas Southwestern Medical School at Dallas, Dallas, Texas 75235*

**ABSTRACT** The rate of passive absorption into the intestinal mucosal cell is determined by at least two major diffusion barriers: an unstirred water layer and the cell membrane. This study defines the morphology and permeability characteristics of these two limiting structures. The unstirred water layer was resolved into two compartments: one behaves like a layer of water overlying the upper villi while the other probably consists of solution between villi. The superficial layer is physiologically most important during uptake of highly permeant compounds and varies in thickness from 115 to 334  $\mu\text{m}$  as the rate of mixing of the bulk mucosal solution is varied. From data derived from a probe molecule whose uptake was limited by the unstirred layer, the effective surface area of this diffusion barrier also was determined to vary with stirring rate and equaled only  $2.4 \text{ cm}^2 \cdot 100 \text{ mg}^{-1}$  in the unstirred condition but increased to  $11.3 \text{ cm}^2 \cdot 100 \text{ mg}^{-1}$  with vigorous mixing. This latter value, however, was still only 1/170 of the anatomical area of the microvillus membrane. With these values, uptake rates for a number of passively absorbed probe molecules were corrected for unstirred layer resistance, and these data were used to calculate the incremental free energy changes associated with uptake of the  $-\text{CH}_2-$  ( $-258 \text{ cal} \cdot \text{mol}^{-1}$ ),  $-\text{OH}$  ( $+564$ ), and taurine ( $+1,463$ ) groups. These studies, then, have defined the thickness and area of the un-

stirred layer in the intestine and have shown that this barrier is rate-limiting for the mucosal uptake of compounds such as fatty acids and cholesterol; in addition, the lipid membrane of the microvillus surface has been shown to be a relatively polar structure.

## INTRODUCTION

Adjacent to every biological membrane there exist lamellae of water through which movement of solute molecules is determined only by diffusional forces. Such an unstirred water layer may, in certain circumstances, exert a major portion of the total resistance encountered by a solute during its movement from the bulk extracellular water phase into the cell interior. While the effects of unstirred layers on various transport processes has been appreciated for a number of years (1-9), their profound influence upon absorption across the intestine has only recently been emphasized. It has been shown, for example, that the aqueous diffusion barrier in the small intestine may cause marked alterations in the kinetics of active transport (10) and lead to significant underestimations of passive permeability coefficients (11-13). In addition, the unstirred layer, and not the cell membrane, may be rate-limiting for absorption of such physiologically important compounds as fatty acids and steroids (13, 14).

To correct for unstirred layer effects upon active and passive transport processes so that the permeability characteristics of the limiting lipid membrane may be more precisely described, it is essential, therefore, that the dimensions of the diffusion barrier be accurately defined. In previous work with relatively flat membranes, it was usually assumed that the unstirred water layer is of uniform thickness and has a surface area equivalent to that of the underlying membrane. It is

A portion of this work was presented before the American Federation for Clinical Research and is reported in abstract form in *Clin. Res.* 20: 736, 1972.

Dr. Westergaard was a postdoctoral fellow in Gastroenterology while these studies were undertaken. His current address is Medical Department P, University Hospital, DK-2100 Copenhagen Ø, Denmark. Dr. Dietschy is a Markle Scholar in Academic Medicine.

Received for publication 29 January 1974 and in revised form 24 April 1974.

obvious that such assumptions cannot be applied to a tissue with so complex an anatomy as the intestinal mucosa. While we have obtained preliminary estimates of the dimensions of the unstirred layer in the intestine of the rat (10), the techniques employed were not sufficiently sensitive to allow precise measurement of solute absorption and thickness of the diffusion barrier when the stirring rate could be altered in a systematic and reproducible manner.

To obviate some of these problems, we have recently designed a new chamber that allows measurements to be made under more precisely controlled conditions (15). Using this chamber, we have undertaken the present studies in rabbit jejunum in an attempt (a) to define the nature of the diffusion barrier in the small intestine; (b) to measure accurately the thickness of that portion of the unstirred water layer that overlies the transport sites on the villi under different conditions of stirring; (c) to quantify the effective surface area of this aqueous diffusion barrier at different rates of mixing; (d) to define the relative resistance to uptake contributed by the unstirred water layer and the microvillus membrane during absorption of a series of solute molecules into the mucosal cell; and, finally, (e) with these various experimentally determined values, to calculate the passive permeability coefficients for a series of fatty acids, alcohols, and bile acids and the incremental free energy changes associated with the addition of various substituent groups to the probe molecules.

## METHODS

**Chemicals.** Unlabeled and  $1\text{-}^{14}\text{C}$  labeled saturated fatty acids and alcohols were all >99% pure as supplied by Applied Science Labs, Inc., State College, Pa.  $[1\text{-}^{14}\text{C}]$ Glucose and  $[1\text{-}^{14}\text{C}]$ galactose were obtained from New England Nuclear, Boston, Mass., and unlabeled glucose and galactose came from Sigma Chemical Co., Inc., St. Louis, Mo.  $[24\text{-}^{14}\text{C}]$ Bile acids were obtained from Mallinckrodt Chemical Works, St. Louis, Mo., and unlabeled bile acids were supplied by Steraloids, Inc., Pawling, N. Y. The purity of these latter compounds was checked by thin-layer chromatography (16–18).  $[\text{G-}^3\text{H}]$ Dextran (mol wt 15,000–17,000) from New England Nuclear was used as a nonpermeant marker to estimate adherent mucosal fluid volume. All other compounds were of reagent grade.

**Tissue preparation.** 2–2.5-kg albino New Zealand rabbits were killed by decapitation. A segment of the upper half of the jejunum, usually 10–15 cm in length, was rapidly removed and rinsed with cold saline. The intestine was then opened along the mesenteric border, and the mucosal surface was thoroughly flushed with a jet of cold saline from a syringe to remove visible mucus and detritus. Circular pieces of intestine were then cut out and mounted as a flat sheet in incubation chambers described in detail elsewhere (15). Basically, in these chambers the circular sheets of jejunum were clamped between two plastic plates so that the serosal and mucosal surfaces were exposed to separate incubation solutions through apertures in the plates

1 cm in diameter. The volume of the serosal compartment was small, whereas the intestinal mucosa was exposed to a large volume of buffer in a beaker, which was mixed by a magnetic stirring bar. After the tissue was mounted, the chambers were placed in beakers containing Krebs-bicarbonate buffer at  $4^\circ\text{C}$  and constantly oxygenated by a stream of 5%  $\text{CO}_2$  in oxygen. 1.2 ml of Krebs-bicarbonate buffer was added to the serosal compartment. The mounted tissue preparations were kept at  $4^\circ\text{C}$  in buffer until used in the various experiments. Before incubation, each chamber was transferred to an identical beaker containing oxygenated Krebs-bicarbonate buffer at  $37^\circ\text{C}$  for a preincubation period of 5 min to allow the tissue to equilibrate at this temperature. The preincubation and incubation solutions were mixed at identical stirring rates with circular magnetic bars, and stirring rates were precisely adjusted by means of a strobe light: stirring rates are reported in this paper as the revolutions per minute at which the stirring bar was driven. These same chambers were used for measurement of both the thickness of the unstirred water layer and unidirectional uptake rates of various probe molecules. In a few studies, gallbladder was mounted in these chambers and handled identically.

**Measurement of unstirred water layer thickness.** The thickness of the unstirred water layer was measured according to the method of Diamond (19). Briefly, the technique consists of measuring the change in the transmural potential difference caused when the mucosal surface of the intestine suddenly is exposed to a hyperosmotic solution. The time required to achieve half the new steady-state potential difference,  $t_{1/2}$ , is a function of the thickness of the unstirred water layer,  $d$ , and the diffusivity of the molecule used to induce the change in potential difference,  $D$ . Thus, the thickness of the unstirred water layer can be calculated from the formula

$$d = (D \cdot t_{1/2} / 0.38)^{1/2} \quad (1)$$

In the derivation of this equation, Diamond (19) emphasizes that it is applicable only when the solute is diffusing up to a membrane surface considered, for practical purposes, to be an infinite plane, when  $d$  and  $D$  are essentially independent of the composition of the bulk perfusion solution, and when the concentration-dependent change in potential difference occurs very rapidly relative to the  $t_{1/2}$  of the electrical transient. Each of these points will be dealt with in subsequent sections.

To measure the  $t_{1/2}$  values, the transmural potential difference was monitored continuously by means of salt bridges placed in the serosal and mucosal compartments of the chamber and connected via calomel half-cells to a voltmeter and rapid response chart recorder. To induce a change in the potential difference, the chamber was rapidly transferred from the preincubation solution to another beaker where a solute such as sucrose had been added to the Krebs-

<sup>1</sup>Abbreviations used in this paper:  $C_1$ , concentration of the probe molecule in the bulk aqueous phase;  $C_2$ , concentration of the probe molecule at the aqueous-microvillus interface;  $D$ , free diffusion coefficient;  $d$ , thickness of the unstirred water layer;  $J$ , rate of uptake of the probe molecule normalized to square centimeter of membrane;  $J_a$ , experimentally determined rate of uptake normalized to tissue dry weight;  $P$ , permeability coefficient;  $S_m$ , effective surface area of the microvillus membrane;  $S_w$ , effective surface area of the unstirred layer;  $t_{1/2}$ , time required to achieve half the steady-state potential difference.

bicarbonate buffer to increase its osmolality. After the new steady-state potential difference was achieved, the chamber was transferred back to the preincubation solution: thus, the  $t_1$  could be measured repeatedly for the build-up and decay of the change in potential difference in the same tissue preparation. These values were used to calculate the effective  $d$  under different experimental circumstances, and these thicknesses are reported in micrometers.

**Measurement of unidirectional flux rates.** The method for measurement of unidirectional flux rates with this chamber has been described in detail elsewhere (15). Briefly, after preincubation of the intestinal sample for 5 min at 37°C, the chamber was transferred to another beaker containing buffer to which both the  $^{14}\text{C}$ -labeled probe molecule and  $^3\text{H}$ -labeled nonpermeable marker had been added. The tissue was incubated for exactly 6 or 8 min, after which the incubation was terminated by rapidly removing the chamber from the solution and rinsing it for approximately 2 s in cold saline. The exposed mucosal tissue was then cut out of the chamber with a circular steel punch, divided into two pieces, and blotted on filter paper, after which each half was placed in a tared counting vial. The tissue was dried in an oven overnight and the dry weight determined. The sample was then saponified with NaOH. Scintillation fluid was added, and radioactivity was determined by means of an external standardization technique to correct for variable quenching of the two isotopes (20). When uptake of volatile compounds was measured, this technique was modified slightly. After incubation, the wet weight of each half of the tissue specimen was determined and one piece was then dried for deter-

mination of tissue dry weight in the usual manner. NaOH was added to the other half, the vials were capped tightly, and the tissue was solubilized in a metabolic shaker at 37°C for 20 min. The vials were then cooled in a refrigerator at 4°C for 30 min and scintillation fluid was added. The dry weight of the solubilized sample was obtained from the dry weight: wet weight ratio, calculated from the dried sample of each pair. The rate of uptake ( $J_a$ ) was then calculated after correcting the total tissue  $^{14}\text{C}$  radioactivity for the mass of the probe molecule present in the adherent mucosal fluid: these rates are expressed as the nanomoles of the probe molecule taken up into the mucosa per minute per 100 milligrams dry weight of tissue.

It should be emphasized that in previous experiments (15), we have shown under the conditions of these experiments (a) that the unstirred water layer in the rabbit jejunum becomes uniformly labeled by the marker compound within 6 min even when unstirred, (b) that the rate of tissue uptake is linear with respect to time and, further, this function extrapolates to zero at zero time, (c) that tissue uptake is linear with respect to the concentration in the bulk buffer phase of passively absorbed compounds, (d) that essentially none of the probe molecules utilized in this study is lost into the serosal compartment in incubations of up to 10 min, and (e) that the presence of high concentrations of bile acids in the bulk solution does not alter the permeability characteristics or histology of the rabbit mucosa.

**Determination of mucosal surface area.** To determine several parameters of the anatomical mucosal surface area, three pieces of rabbit jejunum from five rabbits were mounted in the chambers and incubated in Krebs-bicarbonate buffer for 5 min. One segment was then dried overnight to determine tissue dry weight. The two other pieces were fixed in Bouin's solution, imbedded in paraffin, and cut either transversally or longitudinally. The mucosal surface area was then measured by the method of Fisher and Parsons (21).

## RESULTS

Initial experiments were designed to evaluate five technical features of the application of the Diamond method to intestinal use. First, as shown in Fig. 1A, the change in the steady-state potential difference induced by exposure of the jejunal mucosa to hyperosmotic solutions was linear with respect to the sucrose concentration in the mucosal perfusate up to 200 mM. Hence, in all subsequent experiments a sucrose concentration of 150 mM was utilized to measure  $d$ . Second, since it was necessary to measure repetitively these electrical transients in the same intestinal specimen, it also was important to evaluate the effect of repeated exposure of the mucosal surface to hyperosmotic solutions. As shown in Fig. 1B, the change in the steady-state potential difference induced by 200 mM sucrose was essentially constant for 50 min. Third, when the intestine was exposed to hyperosmotic buffer containing 150 mM sucrose, the  $t_1$  of the electrical transients averaged  $12.2 \pm 0.7$  s (Table I), while the  $t_1$  for the decay of the potential difference back to its base-line value equaled  $13.9 \pm 0.9$  s when the tissue was returned

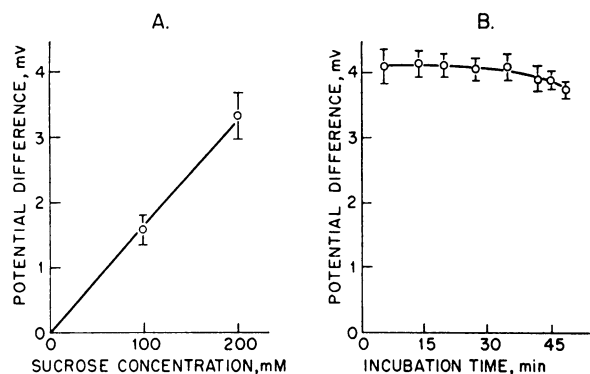


FIGURE 1 The change in the steady-state potential difference across the rabbit jejunum after exposure of the mucosal surface to Krebs-bicarbonate buffer made hyperosmotic with sucrose. A: the incremental change in the potential difference found after incubation of the tissue at two different concentrations of sucrose in the mucosal perfusate. Mean values  $\pm 1$  SEM for specimens obtained from four animals are shown. B: the change in the steady-state potential difference induced in the same samples of intestine whose mucosal surfaces were repeatedly exposed to buffer made hyperosmotic with 200 mM sucrose over a 45-min period. In these studies each tissue sample was exposed to the hyperosmotic fluid until a new steady-state potential difference was achieved, usually about 4 min, and was then returned to isosmotic Krebs-bicarbonate buffer until the next reading was made. Mean values  $\pm 1$  SEM for 15 intestinal segments are shown.

TABLE I  
*d* in Rabbit Intestine Measured with Different  
Probe Molecules

Probe molecules	$D \times 10^6$	$t_1$	$d$
	$\text{cm}^2 \cdot \text{s}^{-1}$	$\text{s}$	$\mu\text{m}$
NaCl	20.3	$5.2 \pm 0.2$	$166 \pm 2.8$ (11)
Urea	17.3	$5.4 \pm 0.3$	$154 \pm 5.0$ (17)
Pentaerythritol	10.2	$8.8 \pm 0.2$	$154 \pm 1.5$ (5)
Alanine	9.3	$8.7 \pm 1.0$	$146 \pm 9.7$ (3)
Mannitol	9.3	$10.4 \pm 0.7$	$157 \pm 5.0$ (15)
Sucrose	7.0	$12.2 \pm 0.7$	$149 \pm 4.1$ (16)
Raffinose	5.8	$14.0 \pm 1.4$	$143 \pm 6.7$ (16)

Electrical transients were measured in jejunal specimens after 30 min of preincubation at 37°C at a stirring rate of 500 rpm. The diffusion potential for NaCl was measured by substituting mannitol isosmotically for NaCl in the mucosal solution to give a serosal/mucosal gradient of 2:1; all other measurements were made with a concentration of 150 mM of the various probe molecules in the mucosal perfusate. Diffusion coefficients were determined as described in reference 13. The figure in parenthesis shows the number of separate intestinal preparations used in each experiment. Mean values  $\pm 1$  SEM are given for the  $t_1$  and thickness of the unstirred water layer,

to isotonic buffer. In all subsequent experiments, only the  $t_1$  values for the build-up of the new steady-state potential difference are reported.

Fourth, in theory the use of sucrose in the intestine to generate a change in potential difference across the mucosa might be invalid, since this compound is hydrolyzed at the brush border, liberating monosaccharides, which in turn could conceivably alter electrical potentials generated by active transport processes in the microvillus membrane. If this were the case, the electrical transient would be a complex function not related in a simple linear fashion to the concentration of the test molecule at the interface. To test the validity of using sucrose, therefore, potential difference changes were induced with several other compounds. As shown in Table I, the  $t_1$  obtained with each different probe molecule varied inversely with its respective free diffusion coefficient, so that the calculated values of  $d$  were all essentially the same. Hence, there was no evidence that the use of sucrose introduced an artifact into the system.

Finally, in initial studies, rhythmic muscular contractions of the mounted jejunal specimens were grossly evident. These contractions introduced artifacts into the tracings of the electrical transients, as can be seen in the example shown in Fig. 2A. However, if the Krebs-bicarbonate buffer in the serosal compartment was replaced by an isotonic solution containing 26 mM potassium, the muscular contractions were inhibited but the  $t_1$  was unaltered (panel B). In a

series of such paired experiments, it was found that high-potassium serosal fluid did not change the calculated value of  $d$  or the value of  $J_a$  for several probe molecules. Hence, in all subsequent experiments dealing with measurements of  $d$ , muscular contraction was inhibited with potassium.

Experiments were next undertaken to characterize the unstirred water layer in a variety of experimental circumstances. The effect of the duration of incubation at a constant stirring rate of the mounted intestinal specimen on the diffusion barrier was first evaluated. As seen in Fig. 3A, after only 5 min of incubation at 37°C, the unstirred layer had an apparent thickness of  $230 \pm 18 \mu\text{m}$  at a stirring rate of 500 rpm; however, with more prolonged incubation in Krebs-bicarbonate buffer,  $d$  became progressively smaller until a constant value of approximately  $155 \mu\text{m}$  was achieved at 30 min of incubation. This finding was in contrast to measurements made simultaneously in the rabbit gall-bladder where, at the same stirring rate,  $d$  remained

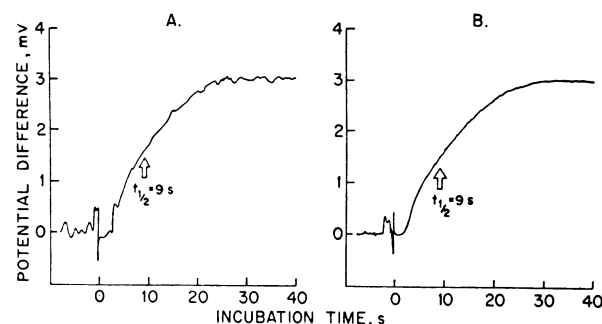


FIGURE 2 The effect of inhibition of muscular contraction of the bowel wall on the  $t_1$  of the electrical transient for the change in the potential difference across the jejunal wall caused by sudden exposure of the mucosa to a hyperosmotic perfusate. Paired specimens of rabbit jejunum were preincubated at 37°C for 30 min with their mucosal surfaces exposed to Krebs-bicarbonate buffer. The serosal compartment of one sample of each pair was filled with Krebs-bicarbonate buffer (A) while the other was filled with an isosmotic solution of NaCl (128 mM) and KCl (26 mM). After this preincubation period the chambers were rapidly transferred to a new mucosal solution of Krebs-bicarbonate buffer made hyperosmotic by addition of 150 mM sucrose, and the change in the transmural potential difference was recorded. The diagrams in this figure represent actual tracings found in one representative pair of intestinal specimens transferred to the hyperosmotic solution at time 0. As can be seen, the irregular artifacts in the tracing of the electrical transient caused by muscular contractions (A) were essentially abolished in the specimen whose serosal surface was exposed to the solution with a high potassium concentration: however, the observed  $t_1$  for the electrical transients and the magnitude of the change in the steady-state potential difference were the same in the two experimental situations.

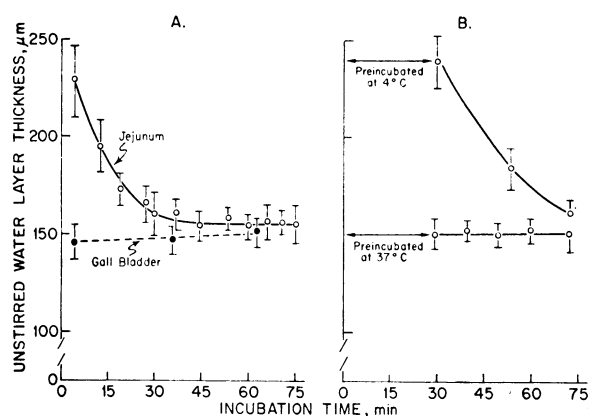


FIGURE 3 The effective  $d$  determined repeatedly in rabbit jejunum and gallbladder incubated in Krebs-bicarbonate buffer. In these studies,  $d$  was measured by suddenly transferring each tissue specimen from Krebs-bicarbonate buffer to buffer made hyperosmotic by the addition of 150 mM sucrose: the stirring rate was kept constant at 500 rpm in all studies. After the electrical transient was recorded and the  $t_3$  determined, the tissue was returned to isosmotic Krebs-bicarbonate buffer until the next measurement was made. A: measurements of  $d$  were made repeatedly in jejunum and gallbladder incubated in buffer at 37°C from the time the tissue was mounted in the chambers. B: paired jejunal specimens from the same animal were preincubated in Krebs-bicarbonate buffer at either 4°C or 37°C for 30 min, at which time the specimen preincubated in the cold was transferred to buffer at 37°C. Repetitive determinations of  $d$  were then made in both types of preparations. Mean values  $\pm$  1 SD are shown for 15 jejunal specimens in each group and for 8 gallbladders.

constant at about 150  $\mu$ m throughout the period of observation.

Not only did the calculated values of  $d$  change in the intestine during a 30-min incubation period, but

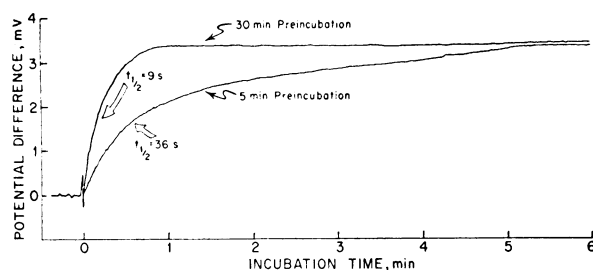


FIGURE 4 The effect of preincubation for 30 min at 37°C on the morphology of the electrical transients. This figure shows the effect of preincubation of the intestine for 30 min at 37°C on the morphology of the electrical transients: two representative tracings are shown superimposed. The change in potential difference was measured in the same sample of jejunum after 5 min and 30 min of incubation at 37°C in Krebs-bicarbonate buffer. As is apparent, essentially the same change in the steady-state potential difference was achieved, but the two curves have markedly different  $t_3$  values.

in addition the morphology of the electrical transients was also significantly altered, as can be seen in the two examples reproduced in Fig. 4. After a 30-min incubation, the electrical transient rapidly reached a maximum value and remained constant thereafter. In contrast, in intestine incubated only 5 min, the transient had an initial rapidly rising phase followed by a very prolonged linear upsweep until a constant steady-state potential difference was finally achieved at about 5 min. Again, this contrasted with the findings in the gallbladder, where the electrical transients at any time during the incubation were of the type seen in intestine after a 30-min incubation.

These findings suggested that some structural alterations might be taking place in the intestinal specimens during prolonged incubation that indirectly were influencing the morphology of the unstirred layer. As shown in Fig. 5, this was found consistently to be the case. After 5 min of incubation (panel A) the central lacteals (CL) were barely visible, and the individual villi were separated by wide intervillus space (IVS). After 30 min of incubation, however, the central lacteals were widely dilated, causing the villi to swell laterally and obliterate the intervillus spaces. It should be noted, however, that the mucosal cells were intact in both instances. In this manner, then, the highly convoluted jejunal mucosa was in essence transformed into an essentially flat surface similar in morphology to that of the gallbladder.

This morphological change could have resulted from solute and water transport into the tightly clamped piece of intestine or, alternatively, from nonspecific damage from repeated exposure to the hyperosmotic test solutions. To differentiate between these two possibilities, samples of jejunum were preincubated in Krebs-bicarbonate buffer for 30 min at a stirring rate of 500 rpm at either 4°C or 37°C;  $d$  was then measured repeatedly, as shown in Fig. 3B. In the intestine preincubated at 37°C, the villi were swollen, the intervillus spaces were closed, and the unstirred layer had a constant thickness of 150  $\mu$ m. In contrast, in the specimens preincubated at 4°C to inhibit solute and water transport, the intervillus spaces were open (as in Fig. 5A) and  $d$  equaled approximately 240  $\mu$ m: with continued incubation at 37°C, however,  $d$  fell to 160  $\mu$ m as histological examination revealed progressive swelling of the villi.

These findings, therefore, were consistent with the view that the value of  $d$  measured in intestine incubated at 37°C for 30 min represented the effective thickness of a superficial layer of unstirred water overlying the upper villi, whereas the value measured in tissue incubated for only 5 min represented a mean value of a very complex unstirred layer, consisting of

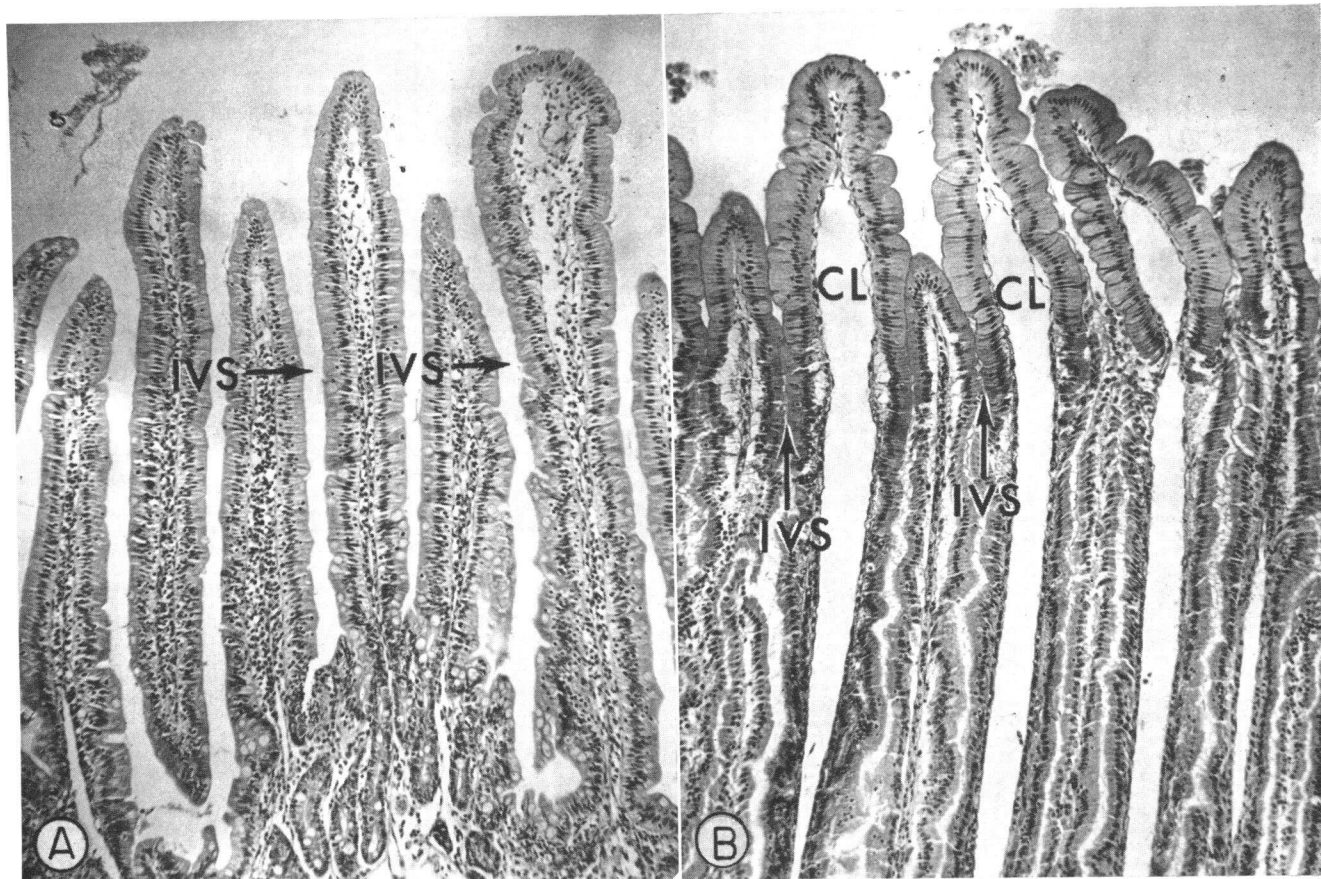


FIGURE 5 The effect of time of tissue incubation at 37°C on the morphology of the mucosal surface of the jejunum. Histological sections were made of paired jejunal specimens preincubated at 37°C for either 5 min (A) or for 30 min (B). As can be seen, the inter-villus spaces (IVS), open at 5 min, became obliterated after 30 min of incubation because of marked dilatation of the central lacteals (CL).

the superficial component plus a deep component interdigitated between the lateral surfaces of the villi. The next series of studies, therefore, was designed to evaluate how the thickness of each of these components varied with the rate of stirring of the bulk mucosal solution. As seen in Fig. 6A, in specimens incubated 5 min and subjected to stirring rates of less than 400 rpm, so much time was required to reach a new steady-state potential difference that accurate  $t_1$  values could not be determined. At higher stirring rates, however, the apparent mean thickness of the total unstirred layer decreased from approximately 300  $\mu\text{m}$  to 220  $\mu\text{m}$ . The superficial component was 334  $\mu\text{m}$  thick in the unstirred condition, and this value decreased in a nearly linear fashion to 160  $\mu\text{m}$  as the stirring rate was increased to 400 rpm: at higher rates of mixing, however,  $d$  approached an essentially constant value of approximately 110  $\mu\text{m}$ . Again, for comparison, the relation of  $d$  in the gallbladder to stirring rate is shown in Fig.

6B. It is apparent that the results obtained for the superficial component in the intestine are essentially superimposable upon those obtained with the gallbladder.

To be able to use these data in calculations involving unstirred layer effects, it was necessary to define which values approximated the thickness of the unstirred layer overlying the physiologically important sites of absorption on the villi. To this end, uptake rates for a variety of probe molecules were measured at a stirring rate of 600 rpm in pairs of intestinal samples, one incubated for 5 min and the other for 30 min at 37° before determination of  $J_a$ . As seen in Table II, for nine passively absorbed probe molecules of widely varying permeation rates, there were no significant differences in the rates of uptake into jejunal samples whether the intervillus spaces were open (5-min preincubation) or closed (30-min preincubation). There was, however, slight depression of uptake of the two

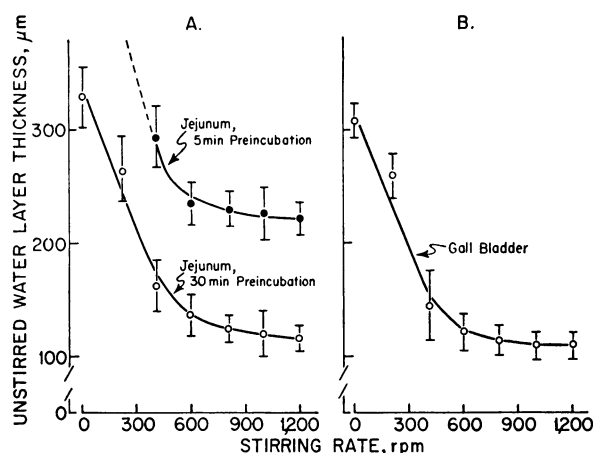


FIGURE 6 The effect of the stirring rate of the bulk mucosal solution on the effective thickness of the superficial and total unstirred water layer in the jejunum.  $d$  was measured at stirring rates that varied from 0 rpm to 1,200 rpm in paired specimens of jejunum preincubated at 37°C for either 5 min or 30 min (A). For comparison, the thickness of the unstirred water layer also was measured at these same stirring rates in the gallbladder (B). Mean values  $\pm 1$  SD are shown for tissues from six animals in each group.

actively transported sugars when the intervillus spaces were occluded. These data strongly suggest that under the conditions of these studies, most absorption, or at least most passive uptake, takes place in the upper portions of the villi and, therefore, the thicknesses determined for the superficial component of the unstirred layer are most appropriate in the mathematical treatment of absorption data.

To obtain transport data that would allow calculation of the permeability characteristics of the microvillus membrane as well as of the effective surface area of the unstirred water layer, two sets of flux rate measurements were next obtained. First, based on paired intestinal specimens,  $J_a$  values, normalized to a bulk phase concentration of 1 mM, were measured for a series of fatty acids, alcohols, and bile acids: these measurements were made in one specimen at a stirring rate of 0 rpm and in the other at 600 rpm. The results of these studies are given in columns 1 and 3 of Table III. Second, with decanol, a substance whose uptake is limited by the unstirred layer, as the probe molecule, uptake rates were measured at a series of different stirring rates. These values of  $J_a$  are shown in Fig. 7A and are plotted against the mean value of  $d$  for the superficial unstirred layer appropriate for the degree of stirring at which each uptake rate was measured (Fig. 6A and Table IV).

Finally, with histological preparations of jejunal specimens incubated identically, three different param-

eters of the anatomical surface area were determined and are given in the lower section of Table IV. 100 mg dry wt of jejunum contained a mucosal cell surface area of 78.9 cm<sup>2</sup>. Assuming that the microvilli increased this area by a factor of 24 (22) the actual area of the luminal cell membrane was approximately 1894 cm<sup>2</sup>·100 mg<sup>-1</sup>. The minimum flat surface overlying the villus tips, i.e., the area of the circular opening in the chamber, equaled 3.2 cm<sup>2</sup>·100 mg<sup>-1</sup>.

## DISCUSSION

As a molecule is passively absorbed from the bulk aqueous solution of the intestinal contents into the cytosol of the mucosal cell, it must cross two major diffusion barriers: the unstirred water layer external to the cell and the protein-lipid membrane of the microvilli. The rate of movement,  $J$ , of the molecule across the unstirred layer is given by the formula

$$J = (C_i - C_s) (D/d) \quad (2)$$

where  $C_i$  and  $C_s$  equal the concentration of the solute in the bulk aqueous phase and at the aqueous-microvillus interface, respectively,  $D$  is the free diffusion coefficient

TABLE II  
Effect of Preincubation for 30 Min on Active and Passive Jejunal Uptake

Test molecule	Jejunal uptake after preincubation	
	5 min	30 min
<i>nmol·min<sup>-1</sup>·100 mg<sup>-1</sup></i>		
Active		
Glucose	178.7 $\pm$ 19.1	133.3 $\pm$ 11.0
Galactose	178.1 $\pm$ 17.6	153.3 $\pm$ 16.8
Passive		
FA 2:0	10.0 $\pm$ 1.2	10.8 $\pm$ 1.5
FA 6:0	23.0 $\pm$ 2.0	26.6 $\pm$ 3.4
FA 8:0	23.7 $\pm$ 1.3	19.7 $\pm$ 2.7
FA 10:0	69.8 $\pm$ 3.4	63.4 $\pm$ 4.4
FA 12:0	132.6 $\pm$ 4.2	130.8 $\pm$ 8.2
Taurocholate	1.0 $\pm$ 0.3	1.3 $\pm$ 0.4
Taurodeoxycholate	5.4 $\pm$ 0.9	4.2 $\pm$ 0.8
Cholate	16.6 $\pm$ 1.4	17.0 $\pm$ 0.4
Deoxycholate	32.1 $\pm$ 3.6	32.7 $\pm$ 2.8

Paired samples of jejunal mucosa were preincubated at 37°C for either 5 or 30 min before determination of absorption rates. Rates of uptake of glucose and galactose were measured from mucosal solutions containing 15-mM concentrations of these sugars. All other uptake rates were measured at 0.25–1.0 mM concentrations of the test molecules; however, uptake rates were all normalized to a concentration of 1.0 mM. Solutions were stirred at 600 rpm. There were 10 pairs of jejunal samples used in each experiment. Mean value $\pm 1$  SEM are given. FA, fatty acid.

TABLE III  
Uptake Rates for Various Test Molecules at Two Different Stirring Rates

Test molecule	Stirring rate 0 rpm		Stirring rate 600 rpm		
	$J_d$	$\frac{J_d}{D} \times 10^{-3}$	$J_d$	$\frac{J_d}{D} \times 10^{-3}$	
	$\text{nmol} \cdot \text{min}^{-1} \cdot 100 \text{ mg}^{-1}$	$\text{nmol} \cdot \text{cm}^{-2} \cdot 100 \text{ mg}^{-1}$	$\text{nmol} \cdot \text{min}^{-1} \cdot 100 \text{ mg}^{-1}$	$\text{nmol} \cdot \text{cm}^{-2} \cdot 100 \text{ mg}^{-1}$	
Saturated fatty acids (FA)					
FA 4:0	(15)	17.8±0.2	24.5	21.4±1.4	29.5
FA 5:0	(9)	11.7±0.9	17.9	16.2±1.7	24.8
FA 6:0	(20)	15.3±0.7	24.3	25.1±1.9	39.8
FA 7:0	(9)	10.2±1.1	16.6	23.4±0.9	38.2
FA 8:0	(8)	12.0±1.3	21.1	27.4±4.8	48.2
FA 9:0	(9)	15.7±1.3	29.4	44.9±1.0	84.0
FA 10:0	(11)	24.9±2.2	49.4	64.0±2.6	127.0
FA 12:0	(8)	32.2±2.6	71.5	125.9±6.4	276.5
Saturated alcohols (Alc)					
Alc 6:0	(4)	32.1±1.8	46.1	100.7±2.7	144.7
Alc 8:0	(4)	43.2±3.9	72.7	206.5±13.9	347.6
Alc 10:0	(4)	37.2±1.1	71.3	433.7±10.6	830.9
Alc 12:0	(4)	35.2±3.0	76.1	369.8±15.2	800.4
Bile acids					
Taurocholate	(10)	—	—	1.3±0.4	3.9
Taurodeoxycholate	(10)	—	—	4.2±0.8	12.3
Cholate	(10)	—	—	17.0±0.4	45.0
Deoxycholate	(10)	—	—	32.7±2.8	85.2

$J_d$  were determined from solutions containing 0.25–1.0-mM concentrations of the test molecules, but all were normalized to a concentration of 1.0 mM. In these experiments one of a pair of jejunum samples from one animal was incubated at a stirring rate of 0 rpm while the other was incubated at a stirring rate of 600 rpm. To calculate the quantity  $J_d/D$ , values of  $D$  for the fatty acids, bile acids, and alcohols were obtained as described in Ref. 13. The figure in parenthesis gives the number of paired observations. Mean values±1 SEM are shown.

for the molecule, and  $d$  represents the effective thickness of the aqueous diffusion barrier. The rate of movement of the molecule across the microvillus membrane equals

$$J = (P)(C_s) \quad (3)$$

where  $P$  is the permeability coefficient of the passively absorbed molecule.

It is apparent from Eq. 3 that any description of the permeability characteristics of the microvillus membranes in terms of  $P$  requires knowledge of the concentration of the probe molecule at the aqueous-lipid interface, i.e., at  $C_s$ . By rearranging Eq. 2, this value can be calculated by the formula

$$C_s = C_i - J(d/D) \quad (4)$$

where the term  $J(d/D)$  represents the reduction in the concentration of the probe molecule caused by the resistance that it encounters in traversing the unstirred water layer. However, in this as well as in the pre-

ceding equations, the flux term,  $J$ , must have the units of mass·unit time<sup>-1</sup>·area (in centimeters)<sup>-2</sup>. Experimentally determined flux rates, however, commonly are normalized to tissue dry or wet weight, unit length (in the case of intestine), unit protein or DNA, or the area of the membrane exposed in a particular incubation chamber. In none of these instances, therefore, are the flux rates normalized to the proper surface area term: such values, therefore, cannot be substituted directly into these various equations.

In the present studies, the experimentally determined uptake rates,  $J_d$ , have the units nanomoles·minute<sup>-1</sup>·100 milligrams dry weight<sup>-1</sup>. To utilize such data to correct for unstirred layer resistance, it is necessary to know a conversion factor that gives the effective surface area of the unstirred water layer through which a particular mass of probe molecules moves, i.e., the area of the unstirred layer overlying an amount of jejunum having a dry weight of 100 mg. For the purposes of this study we have designated this con-



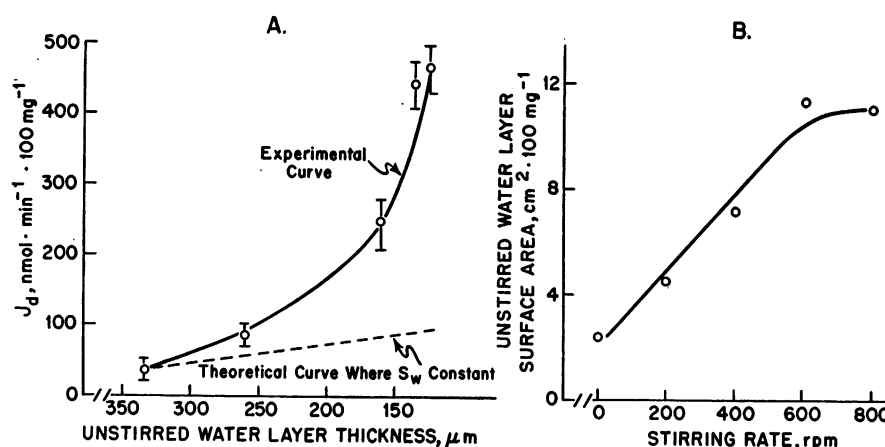


FIGURE 7 The effect of the stirring rate of the bulk mucosal solution on the uptake of [ $^{14}\text{C}$ ]decanol into the jejunum and on the effective surface area of the unstirred water layer. Decanol absorption was measured at five different stirring rates that varied from 0 to 800 rpm. A: the  $J_d$  of this compound are plotted against the determined  $d$  appropriate for each particular rate of stirring as taken from Fig. 6A and Table IV. The dashed line shows the theoretical values of  $J_d$  as a function of the  $d$ , if the surface area of this diffusion barrier,  $S_w$ , remained constant at all degrees of stirring. B: the mean values of  $S_w$  at each rate of stirring calculated from the experimental data on decanol uptake as described in the text. The experimental values in A represent mean  $\pm 1$  SEM for five animals.

TABLE IV  
 *$S_w$  in the Jejunum Compared to the Anatomical Surface Area of the Mucosa*

$S_w$ at different stirring rates		
Stirring rate	$d$	$S_w$
rpm	$\mu\text{m}$	$\text{cm}^2 \cdot 100 \text{ mg}^{-1}$
0	$334 \pm 16$	2.4
200	$262 \pm 13$	4.4
400	$160 \pm 6$	7.7
600	$137 \pm 3$	11.7
800	$125 \pm 4$	11.3
Anatomical area of the jejunum		
Parameter	Area	
	$\text{cm}^2 \cdot 100 \text{ mg}^{-1}$	
Minimum flat surface	3.2	
Mucosal surface	78.9	
Mucosal surface + microvilli	1,894.0	

$S_w$  were calculated as described in the text from data on the uptake of decanol at different stirring rates. Values for  $d$  at these same stirring rates also are shown and are derived from the data shown in Fig. 6A. Anatomical surface area parameters were measured from incubated specimens as described by Fisher and Parsons (21). The minimum flat surface area corresponds to the area of the circular aperture in the retaining plate of the incubation chamber. The other two values correspond to the area of the mucosal surface without and with the microvilli taken into consideration.

version factor as  $S_w$  and it has the units square centimeters per 100 milligrams. Thus, in calculations of movement of solute across the aqueous diffusion barrier, it is apparent that the term  $J_d/S_w$  is equal to  $J$ , since by this manipulation the experimentally determined flux rates can be reduced to the appropriate units, i.e., nanomoles  $\cdot$  second $^{-1}$   $\cdot$  centimeters $^{-2}$ . Eq. 4, therefore, can be rewritten

$$C_2 = C_1 - \frac{(J_d)(d)}{(S_w)(D)} \quad (5)$$

Similarly, in calculations dealing with movement of probe molecules across the microvilli, it also is necessary to know the effective surface area of this membrane. For this purpose we have designed the term  $S_m$  to represent the area of lipid membrane across which an observed flux,  $J_d$ , has occurred in an amount of jejunum equivalent to 100 mg dry wt. By appropriate substitution of this constant into Eq. 3 and after rearranging terms, the permeability coefficient for a particular passively absorbed solute is given by the expression

$$P = \frac{J_d}{(C_2)(S_m)} \quad (6)$$

It is apparent from these considerations that an accurate appraisal of the permeability characteristics of the microvillus membrane in the intestine cannot be undertaken without precise information on the thickness of

the unstirred water layer,  $d$ , the effective surface area of the unstirred layer,  $S_u$ , and the effective surface area of the microvillus membrane,  $S_m$ .

Initial experiments in the present study, therefore, were designed to investigate the nature and dimensions of the unstirred water layer. Preliminary measurements suggested that the diffusion barrier was several hundred micrometers thick. However, the intestinal mucosa contains two structural elements, mucus and glycocalyx, overlying the microvillus membrane that could conceivably lead to artifacts in determination of  $d$ . If either of these elements slowed diffusion of the probe molecule up to the lipid membrane, it would result in an overestimation of the thickness of the unstirred layer. However, several lines of evidence suggest that this is not the situation. For example, if some structural element outside the cell membrane contributed significant resistance to free diffusion of the test molecules, then one might reasonably expect that this barrier would discriminate among molecules of different size or charge. As seen in Table I, this was not the case: the diffusion barrier did not discriminate between molecules whose molecular weight varied from 26 to 600 daltons and which were either charged or uncharged. Furthermore, unstirred water layers of similar dimensions have been found in other biological membranes, such as gallbladder (6, 19), which have much less prominent mucus and glycocalyx layers, and in artificial membranes that have no mucus or glycocalyx at all (23). We have concluded, therefore, for the purposes of all subsequent calculations, that the diffusion barrier is in fact principally a layer of unstirred water.

The applicability of the Diamond method for measurement of the functional thickness of the unstirred layer depends critically upon the validity of several assumptions with respect to the characteristics of this barrier in the intestine (19). First, the properties of the unstirred layer must not change with alterations in the composition of the bulk perfusate. As noted in Table I, this appears to be the case, since  $d$  was essentially constant under all circumstances tested. Second,  $D$  for the probe molecule used to induce the change in potential difference must be essentially constant throughout the concentration range utilized. Again this was true in the present experiments. For example,  $D$  for sucrose in 150 mM NaCl only varies from  $6.9 \times 10^6$  cm<sup>2</sup>·s<sup>-1</sup> at infinite dilution to  $6.2 \times 10^6$  cm<sup>2</sup>·s<sup>-1</sup> at 150 mM—a variation that would not introduce a quantitatively significant error into the calculation of  $d$  (24). Third, any permeability changes in the membrane induced by the build-up of the concentration of the probe molecule at the interface must occur very rapidly relative to the time-course of the electrical transient.

The fact that  $d$  measured under isosmotic conditions from the electrical transient of the diffusion potential generated from a NaCl gradient was nearly the same as the values obtained with all of the other probe molecules again suggests that this condition was met in the intestine.

The fourth assumption inherent in the derivation of Eq. 1 is that the probe molecule diffuses from the bulk solution up to a flat membrane considered for practical purposes to be an infinite plane. Obviously this condition is not met when the intervillus spaces are open. After 30 min of incubation, however, when the intervillus spaces are fully occluded, four lines of evidence suggest that the intestinal mucosal surface could be considered as an essentially flat plane similar in morphology to the mucosa of the gallbladder. First, the gradual decrease in  $d$  seen during the incubation of jejunum (Fig. 3A) was very likely the result of obliteration of the deep components of the unstirred layer as the villi swelled and was not related to other nonspecific effects of prolonged incubation, since unstirred-layer thicknesses measured simultaneously in the gallbladder were unchanged throughout this period of observation. Gallbladder epithelium lacks villi: thus, in contrast to the situation in the intestine, even though submucosal edema developed in these specimens, essentially no change should occur in the dimensions of the overlying diffusion barrier. Second, beyond 30 min of incubation,  $d$  approached a constant value essentially the same as that measured under the same conditions in the gallbladder (Fig. 3A). Third, as seen in Fig. 6, the thickness of the diffusion barrier overlying jejunum preincubated for 30 min diminished in response to increased stirring of the bulk mucosal solution, as in the gallbladder. This was true in terms of both the profile of the curves relating  $d$  to stirring rate and the absolute values of  $d$  at any particular rate of mixing. Finally, the morphology of the electrical transients, as seen in Fig. 4, changed during the 30-min period of incubation. Initially, they manifested a long terminal linear phase compatible with diffusion of the probe molecules down the long channels between villi, whereas after 30 min of incubation, the transients resembled those anticipated when the sucrose was diffusing up to a flat membrane and which, in fact, were consistently seen in recordings from gallbladder.

We have concluded, therefore, that the  $t_1$  values of the electrical transients measured in jejunal specimens preincubated for 30 min can be translated into valid measurements of the thickness of the superficial unstirred water layer overlying the upper villi. In addition, since the data reported in Table II indicate that passive uptake of a variety of probe molecules occurs in this same region of the intestinal villi, we have

further concluded that these measurements provide the appropriate values of  $d$  for use in considerations of passive transport processes in the intestine: as shown by the lower curve in Fig. 6A, these values vary from  $334 \pm 16 \mu\text{m}$  in the unstirred situation to  $112 \pm 12 \mu\text{m}$  at a high stirring rate of 1,200 rpm.

The next problem of major importance was to arrive at values for  $S_w$  and, further, to establish whether this parameter, like  $d$ , varied with the stirring rate. Such information can be obtained from the values of  $d$  given above and the passive flux rates determined for the various probe molecules and shown in Table III. By substituting the quantity  $J_a/S_w$  for  $J$  in Eq. 2, this expression may be rewritten.

$$J_a/S_w = (C_1 - C_2)(D/d) \quad (7)$$

This equation has two unknowns,  $C_2$  and  $S_w$ . However, in the special circumstance where  $J_a$  is measured for a probe molecule whose uptake is totally limited by the unstirred water layer,  $C_2$  becomes essentially equal to zero and can be deleted from the equation; hence, after solving for  $S_w$ , we obtained the following expression.

$$S_w = \frac{(J_a)(d)}{(C_1)(D)} \quad (8)$$

This equation, then, allows calculation of  $S_w$  in terms of the known quantities  $J_a$ ,  $d$ ,  $C_1$ , and  $D$ ; it must be emphasized, however, that this expression yields valid values only when  $J_a$  is measured for a probe molecule that penetrates the microvillus membrane very much faster than it moves across the unstirred water layer, i.e., a molecule that has a value of  $P \gg \gg D/d$ . Such molecules can be identified in Table III by dividing the observed value of  $J_a$  for each compound by its appropriate free diffusion coefficient, as has been done in columns 2 and 4. As is apparent, as one goes from the more polar to the less polar members of these homologous series, the rate of penetration of the cell membrane becomes much greater than the rate of diffusion across the unstirred water layer and, therefore,  $J_a$  becomes proportional to  $D$  and the quantity  $J_a/D$  reaches a constant value. In the unstirred situation, four compounds achieved an essentially constant value for this quantity in the range of 71.3–76.1  $\text{nmol} \cdot \text{cm}^{-2} \cdot 100 \text{ mg}^{-1}$ ; these included the 12:0 fatty acid and the 8:0, 10:0, and 12:0 alcohols. At a stirring rate of 600 rpm, however, where unstirred layer resistance was much less, only the 10:0 and 12:0 alcohols plateaued at a constant value. Thus, since decanol uptake was clearly limited by the unstirred layer in both the unstirred and stirred situations, this probe molecule was used to quantify  $S_w$ .

To this end, decanol uptake was systematically measured at stirring rates varying from 0 to 800 rpm. In this range of stirring, the superficial unstirred layer varied in thickness from 334 to 125  $\mu\text{m}$ , as tabulated in Table IV. If the effective surface area of the unstirred layer remained constant at all stirring rates, then decanol uptake should vary in an inverse, linear manner with  $d$ ; this theoretical relationship is illustrated by the dashed line in Fig. 7A. It is apparent, however, that the experimentally determined values progressively deviated from the theoretical values as the stirring rate was increased and the effective thickness of the unstirred layer decreased; this finding indicated that the effective surface area of the unstirred layer also was altered by stirring.

By substituting these values of  $J_a$  for decanol at each of the five stirring rates, along with the appropriate values of  $d$  for the superficial unstirred layer in Eq. 8, the effective surface area,  $S_w$ , was calculated to vary from 2.4 to 11.3  $\text{cm}^2 \cdot 100 \text{ mg}^{-1}$  as the stirring rate was varied from 0 to 800 rpm (Table IV).

These values may now be compared with several parameters of the anatomical surface area in these same jejunal samples. In the unstirred situation where  $d$  is very large, it would be anticipated that decanol would be totally absorbed at the villus tips and, therefore, would traverse a minimal surface area of the unstirred layer. As seen in Table IV, this was the case:  $S_w$  equaled 2.4  $\text{cm}^2 \cdot 100 \text{ mg}^{-1}$ , which corresponds almost exactly to that portion of the minimum flat anatomical surface area (3.2  $\text{cm}^2 \cdot 100 \text{ mg}^{-1}$ ) occupied by villus tips. At the other extreme, at a stirring rate of 800 rpm  $S_w$  increased so as to correspond to approximately 1/7 of the mucosal surface of the villi, i.e.,  $S_w$  equaled 11.3  $\text{cm}^2 \cdot 100 \text{ mg}^{-1}$  versus a mucosal surface area of 78.9  $\text{cm}^2 \cdot 100 \text{ mg}^{-1}$ .

These data, then, provide information concerning the dimensions of the unstirred diffusion barrier in the small intestine which allows several major conclusions of physiological importance to be drawn about passive absorption into the mucosal cell. These conclusions deal with the relative resistance encountered by different solutes in crossing the unstirred water layer and the lipid-protein membrane of the microvilli.

First, it is apparent that there is a large group of solutes of major physiological importance capable of penetrating the cell membrane much faster than the unstirred water layer. This conclusion derives from the data presented in Fig. 8: in this diagram the natural logarithm of  $J_a$  of each fatty acid and alcohol given in Table III divided by its appropriate  $D$  has been plotted against chain length. In this type of plot those members of the homologous series whose uptake is limited by diffusion through the unstirred water layer will

manifest no increase in  $J_a/D$  with increasing chain length, i.e., the slope will equal zero. In contrast, those molecules whose uptake is predominantly limited by the cell membrane will show an increase in  $J_a/D$  that is essentially log-linear with chain length: this relationship exists because the addition of each  $-\text{CH}_2-$  group to the molecule increases the permeation rate of the cell membrane by a constant factor (25). As is apparent in Fig. 8, at the high stirring rate where unstirred layer resistance is low, uptake of fatty acids 7:0 through 12:0 is principally limited by the cell membrane. The short chain-length fatty acids 4:0, 5:0, and 6:0 manifest higher rates of uptake than would be anticipated from a linear extrapolation of the relationship for the longer chain-length fatty acids. Such deviant behavior has been found for a number of other low molecular-weight, very polar compounds in a variety of epithelial membranes, and may result from movement of these molecules through low-resistance shunt pathways between cells or because of some unusual permeability characteristic of the microvillus membrane itself (13, 25–30). Uptake of the alcohols is much more rapid than the corresponding acids: however, the relative increase in permeation for the addition of each  $-\text{CH}_2-$  group is the same up to decanol. At this point, the unstirred layer apparently becomes rate-limiting. As shown in Fig. 8A, in the unstirred situation where unstirred layer resistance is much greater, this diffusion barrier becomes rate-limiting to mucosal uptake of octanol and all longer chain-length alcohols and even for the 12:0 fatty acid. When the unstirred layer becomes totally rate-limiting,  $C_s$  must equal essentially zero. In this special case, the limiting value of  $J_a/D$  can be calculated by rearranging Eq. 8. With the values of  $d$  and  $S_w$  from Table IV appropriate for a stirring rate of 0 and 600 rpm,  $J_a/D$  equals  $72 \times 10^8 \text{ nmol} \cdot \text{cm}^{-2} \cdot 100 \text{ mg}^{-1}$  and  $854 \times 10^8 \text{ nmol} \cdot \text{cm}^{-2} \cdot 100 \text{ mg}^{-1}$ , respectively. These limiting values are shown as dashed lines in Fig. 8.

The major conclusion to be drawn from these considerations is that the unstirred water layer, and not the microvillus membrane, is rate-limiting to the uptake of long-chain fatty acids and other nonpolar compounds, such as cholesterol. While the limiting value of  $J_a/D$  has not yet been measured in vivo, several lines of indirect evidence would suggest that the value of the ratio  $S_w/d$  is very low, so that unstirred layer resistance is high in the intact animal. It is apparent, therefore, that variations in lipid absorption among different animal species or in different disease states may reflect, in part, variations in unstirred layer resistance. Furthermore, the precise role of the bile acid micelle in facilitating lipid uptake must be explained in

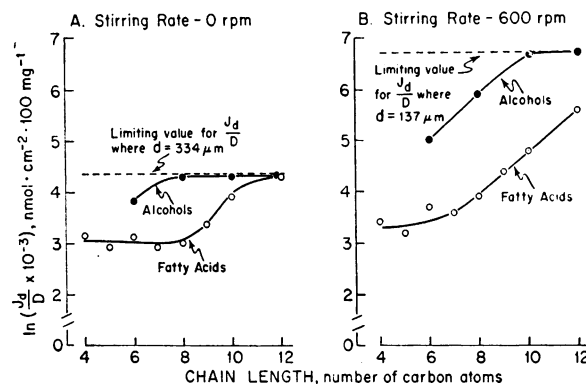


FIGURE 8 The relationship between the rates of uptake of a homologous series of fatty acids and alcohols and the number of carbon atoms in each compound. In these two panels the  $\ln$  of the quantity  $J_a/D \times 10^{-8}$  determined for a series of fatty acids and alcohols (Table III) is plotted as a function of the chain length of each compound. A and B show such data in the unstirred and stirred (600 rpm) situation, respectively. In addition, the two limiting values have been calculated, as described in the text, which denote the maximum rates of passive uptake at the two stirring rates that any compound can achieve: at these rates the unstirred water layer becomes absolutely rate-limiting to absorption.

terms of overcoming the resistance of this diffusion barrier (31).

The second major set of data that can be derived from these studies concerns the permeability characteristics of the microvillus membrane as expressed in terms of the absolute permeability coefficients for a number of probe molecules, and in terms of the incremental free energies of solution associated with the addition of various substituent group to the probe molecules. By using Eq. 5, the concentration of each test molecule at the microvillus interface was calculated from the  $J_a$  values measured at a stirring rate of 600 rpm (Table III) with values of  $11.7 \text{ cm}^2 \cdot 100 \text{ mg}^{-1}$  and  $137 \mu\text{m}$ , respectively, for  $S_w$  and  $d$ : these values of  $C_s$  are shown in the second column of Table V.<sup>a</sup> By

<sup>a</sup>In the preceding calculations dealing with diffusion-limited uptake, the values of  $d$  and  $S_w$  given in Table IV are appropriate, since they were derived specifically for the situation where  $C_s$  for the probe molecules approached 0. It does not necessarily follow, however, that these values are appropriate for molecules whose uptake is primarily membrane-limited, so that  $C_s$  more closely approaches  $C_i$  than 0. It is reasonable to assume, therefore, that for these compounds  $S_w$  might be slightly greater than  $11.7 \text{ cm}^2 \cdot 100 \text{ mg}^{-1}$ . However, as is apparent in Eq. 5, the correction factor depends upon the ratio of  $d$  to  $S_w$ , not necessarily the absolute value of either of these: thus, for the conditions assumed above,  $d/S_w$  equals  $1.17 \times 10^{-8} \text{ 100 mg} \cdot \text{cm}^{-1}$ . If a larger surface area is involved in the absorption of these less permeant compounds, then it is likely that the mean value of  $d$  also would increase as the molecules move further down between villi, so that the ratio would

correcting each flux rate for the appropriate value of  $C_2$ , the first set of permeability coefficients, shown in the third column of Table V, were obtained. These values, however, are normalized to 100 mg tissue dry weight: in order to obtain  $P$  values normalized to the area of the microvillus membrane, a value for  $S_m$  was required. If the effective surface area of the unstirred water layer in this experimental circumstance equals  $11.7 \text{ cm}^2 \cdot 100 \text{ mg}^{-1}$ , and if the microvillus folds increased the area of the mucosal cell membrane by a factor of 24, then  $S_m$  should equal approximately  $208.8 \text{ cm}^2 \cdot 100 \text{ mg}^{-1}$  (22). With this value, the second set of permeability coefficients, shown in the last column of Table V, were obtained. Obviously this calculation assumes that all of the microvillus membrane participates in this absorptive process. The calculated permeability coefficients, therefore, are minimum values.

The permeability characteristics of the intestinal brush border also can be described in terms of the relative effect on permeation of the addition of specific substituent groups to the probe molecules. For example, when the logarithm of either set of permeability coefficients is plotted as a function of chain length for the fatty acids 7:0 through 12:0 and the alcohols 6:0 and 8:0, the slopes of the best fit straight lines correspond to an average increase in  $P$  by a factor of 1.52 for each  $-\text{CH}_2-$  group added to the chain. This, in turn, equals an incremental free energy change,  $\delta\Delta F_{w \rightarrow i}$ , of  $-258 \text{ cal} \cdot \text{mol}^{-1}$  (25). By the permeability data for the four bile acids, the addition of a  $-\text{OH}$

remain relatively constant. The validity of this assumption and the magnitude of the potential errors inherent in these calculations can be tested by determining the effect of reasonable variations in  $d/S_w$  on the semilogarithmic plot of  $P$  against chain length for the fatty acids 7:0 through 12:0: the corrected value of this ratio should yield a straight line relationship. Consider first the situation, where  $d/S_w$  is two-fold greater, i.e., equals  $2.34 \times 10^{-3} 100 \text{ mg} \cdot \text{cm}^{-1}$ . This situation is very unlikely, since it would imply that these less permeant molecules are transversing an unstirred layer where either  $S_w$  is smaller relative to  $d$  or, alternatively, where  $d$  is disproportionately larger relative to  $S_w$ , than is true for molecules whose uptake is completely diffusion-limited. Indeed, when this value is used,  $\ln P$  is not linear with respect to chain length but rather the curve turns sharply upward, indicating an inappropriate overcorrection for unstirred layer resistance. The more likely possibility is that  $d/S_w$  is less than  $1.7 \times 10^{-3} 100 \text{ mg} \cdot \text{cm}^{-1}$ , since this would imply that for these molecules  $S_w$  should be increased by an amount disproportionately larger than the appropriate increase in  $d$ . However, even when  $S_w$  is assumed to be two-fold larger so that  $d/S_w$  equals  $0.59 \times 10^{-3} 100 \text{ mg} \cdot \text{cm}^{-1}$ , the calculated permeability coefficients are reduced only slightly below those given in Table V. Hence, while there is some uncertainty as to the values of  $d$  and  $S_w$  that are appropriate for passively absorbed molecules of low permeability, this uncertainty introduces only minor errors into the calculations of  $P$ .

TABLE V  
Calculation of Corrected Permeability Coefficients

Test molecule	$(J_d)(d)$		$P$	$P \times 10^6$
	$(S_w)(D)$	$C_2$		
	<i>mM</i>	<i>mM</i>	$\text{nmol} \cdot \text{min}^{-1} \cdot 100 \text{ mg}^{-1} \cdot \text{mM}^{-1}$	$\text{cm} \cdot \text{s}^{-1}$
Saturated fatty acids (FA)				
FA 4:0	0.03	0.97	22.4	1.79
FA 5:0	0.03	0.97	16.7	1.33
FA 6:0	0.05	0.95	26.4	2.11
FA 7:0	0.04	0.96	24.4	1.95
FA 8:0	0.05	0.95	28.8	2.30
FA 9:0	0.10	0.90	49.9	3.98
FA 10:0	0.14	0.86	74.4	5.94
FA 12:0	0.32	0.68	185.1	14.77
Saturated alcohols (Alc)				
Alc 6:0	0.16	0.84	119.9	9.57
Alc 8:0	0.40	0.60	344.2	27.47
Bile acids				
Taurocholate	0.00	1.00	1.3	0.10
Taurodeoxycholate	0.01	0.99	4.2	0.34
Cholate	0.06	0.94	18.1	1.44
Deoxycholate	0.11	0.89	36.7	2.93

To calculate  $P$  for the various probe molecules, the experimentally determined  $J_d$  obtained at a stirring rate of 600 rpm, shown in the third column of Table III, were corrected for unstirred layer resistance as described in the text. The correction term for the unstirred layer effect,  $(J_d)(d)/(S_w)(D)$ , shown in the first column, was calculated with a value of  $11.7 \text{ cm}^2 \cdot 100 \text{ mg}^{-1}$  for  $S_w$  and  $137 \text{ } \mu\text{m}$  for  $d$  (Table IV).  $D$  was obtained as described in ref 13. The calculated concentrations of each probe molecule at the aqueous-lipid interface, i.e., at  $C_2$ , is given in the second column. Two different sets of  $P$  were calculated and are shown in the third and fourth columns. The first group was normalized to tissue dry weight. These were calculated for each probe molecule by dividing its  $J_d$  value at 600 rpm (Table III) by its concentration at the interface,  $C_2$ . In the second group, the  $P$  were normalized to the surface area of the microvillus membrane and were calculated by dividing each permeability coefficient in the third column of this table by  $S_m$ , estimated to equal  $208.8 \text{ cm}^2 \cdot 100 \text{ mg}^{-1}$  in this experimental circumstance, and reducing the units to  $\text{cm} \cdot \text{s}^{-1}$ .

group reduced the rate of uptake by a factor of 0.40 ( $\delta\Delta F_{w \rightarrow i}$ ,  $+564 \text{ cal} \cdot \text{mol}^{-1}$ ) while the substitution of the taurine group for the carboxyl function diminished permeation by a factor of 0.093 ( $\delta\Delta F_{w \rightarrow i}$ ,  $+1,463 \text{ cal} \cdot \text{mol}^{-1}$ ). Finally, in going from an  $\text{R-H}_2\text{COH}$  group to  $\text{R-COO}^-$ , uptake was reduced by a factor of 0.15 ( $\delta\Delta F_{w \rightarrow i}$ ,  $+1,162 \text{ cal} \cdot \text{mol}^{-1}$ ). Thus, the microvillus membrane of the rabbit jejunum, like several other epithelial surfaces recently studied, is a relatively polar structure: more polar, in fact, than bulk isobutanol (6, 12, 13, 25).<sup>3</sup>

<sup>3</sup> The rate of passive penetration of a cell membrane is determined primarily by the membrane:water partition coefficient of a particular solute molecule (25). The relative polarity, therefore, of a particular biological membrane can be judged by comparing the effect of a substituent group on permeation of that membrane with the effect of the group on the lipid:water partition coefficients of the probe molecule with various bulk solvents. For example, the addition of an  $-\text{OH}$  group to a molecule will reduce

These permeability characteristics for the jejunum may be compared with those of another tissue in this species, since Smulders and Wright have recently reported an analysis of both the relative and absolute permeability characteristics of rabbit gallbladder (6). These authors found that the gallbladder epithelium also behaves as if it is more polar than isobutanol: the addition of a -OH group to a probe molecule, for example, reduced permeation by a factor of only 0.49. In addition, the absolute permeability coefficient for 1,6-hexanediol, corrected for the surface area of the luminal epithelial membrane, was  $4.6 \times 10^{-6} \text{ cm} \cdot \text{s}^{-1}$  while in the jejunum this compound would have an expected permeability coefficient of  $3.8 \times 10^{-6} \text{ cm} \cdot \text{s}^{-1}$ .<sup>4</sup> Thus, in both relative and absolute terms these two epithelial surfaces are very similar. Whether these permeability features are characteristic of all mammalian membranes or are peculiar to epithelial surfaces remains an unanswered question of critical importance.

Finally, it should be emphasized that while the values of  $S_w$  and  $d$  derived from these studies are appropriate for considerations of passive absorption, they cannot be utilized for correction of unstirred layer effects on active transport processes in the intestine. It seems a reasonable possibility that active transport sites may be distributed over an area of the mucosal surface different from that involved in passive absorption, so that the mean values of  $S_w$  and  $d$  would differ from those quoted above. Because of the significant effects that unstirred layers may have on the kinetics of active transport (10, 32), however, it is of critical importance that techniques be developed to establish appropriate values for  $S_w$  and  $d$  for carrier-mediated processes.

its partitioning into isobutanol, ether, and olive oil by a factor of 0.197, 0.033, and 0.011, respectively (25). Thus, that the addition of this substituent group reduces the permeability coefficient for probe molecules in the jejunum by a factor of only 0.40 indicates that the microvillus membrane is even more polar than isobutanol.

<sup>4</sup>The permeability coefficient of 1,6-hexanediol reported by Smulders and Wright in gallbladder equaled  $6.4 \times 10^{-5} \text{ cm} \cdot \text{s}^{-1}$  when the flux rate was corrected for unstirred layer resistance and normalized to the area of the chamber (6). However, they estimated that the mucosal folds increased the surface area by a factor of 14; therefore  $P$  for this compound normalized to the surface area of the cell membrane equals  $4.6 \times 10^{-6} \text{ cm} \cdot \text{s}^{-1}$ . These data also allow a comparison between the functional surface areas of the two membranes. In the gallbladder there was  $14 \text{ cm}^2$  cell surface/ $\text{cm}^2$  exposed epithelium. In the jejunum  $S_w$  was considered to equal  $208.8 \text{ cm}^2 \cdot 100 \text{ mg}^{-1}$ ; since the incubation chamber aperture had a surface area of  $0.79 \text{ cm}^2$  and held, on the average, 25 mg dry wt of tissue, this corresponds to  $66 \text{ cm}^2$  absorbing cell surface/ $\text{cm}^2$  of exposed tissue. The permeability coefficient for 1,6-hexanediol in jejunum was calculated by assuming that the addition of one more -OH group to hexanol would reduce its  $P$  value ( $9.57 \times 10^{-6} \text{ cm} \cdot \text{s}^{-1}$ ) by a factor of 0.40.

## ACKNOWLEDGMENTS

These studies were supported by U. S. Public Health Service Research Grants 5 R01 HL09610 and 1 R01 AM-16386, by U. S. Public Health Service Training Grant 5 T01 AM05490 and by a grant from the John and Mary Markle Foundation. Dr. Westergaard was supported by U. S. Public Health Service Fogarty International Research Fellowship 5 F05 TW01808.

## REFERENCES

1. Collander, R. 1954. The permeability of nitella cells to non-electrolytes. *Physiol. Plant.* 7: 420-445.
2. Dainty, J. 1963. Water relations of plant cells. *Adv. Bot. Res.* 1: 279-326.
3. Wedner, H. J., and J. M. Diamond. 1969. Contributions of unstirred-layer effects to apparent electrokinetic phenomena in the gall-bladder. *J. Memb. Biol.* 1: 92-108.
4. Kidder, G. W., III. 1970. Unstirred layers in tissue respiration: application to studies of frog gastric mucosa. *Am. J. Physiol.* 219: 1789-1795.
5. Andreoli, T. E., and S. L. Troutman. 1971. An analysis of unstirred layers in series with "tight" and "porous" lipid bilayer membranes. *J. Gen. Physiol.* 57: 464-478.
6. Smulders, A. P., and E. M. Wright. 1971. The magnitude of nonelectrolyte selectivity in the gallbladder epithelium. *J. Memb. Biol.* 5: 297-318.
7. Hays, R. M., N. Franki, and R. Soberman. 1971. Activation energy for water diffusion across the toad bladder: evidence against the pore enlargement hypothesis. *J. Clin. Invest.* 50: 1016-1018.
8. Gutknecht, J., and D. C. Tosteson. 1973. Diffusion of weak acids across lipid bilayer membranes: Effects of chemical reactions in the unstirred layers. *Science (Wash. D. C.)* 182: 1258-1261.
9. Rey, F., F. Drillet, J. Schmitz, and J. Rey. 1974. Influence of flow rate on the kinetics of the intestinal absorption of glucose and lysine in children. *Gastroenterology* 66: 79-85.
10. Wilson, F. A., and J. M. Dietschy. 1972. The effect of unstirred layers on the kinetics of active transport in the rat intestine. *Clin. Res.* 20: 783. (Abstr.)
11. Dietschy, J. M., V. L. Sallee, and F. A. Wilson. 1971. Unstirred water layers and absorption across the intestinal mucosa. *Gastroenterology* 61: 932-934.
12. Wilson, F. A., and J. M. Dietschy. 1972. Characterization of bile acid absorption across the unstirred water layer and brush border of the rat jejunum. *J. Clin. Invest.* 51: 3015-3025.
13. Sallee, V. L., and J. M. Dietschy. 1973. Determinants of intestinal mucosal uptake of short- and medium-chain fatty acids and alcohols. *J. Lipid Res.* 14: 475-484.
14. Wilson, F. A., V. L. Sallee, and J. M. Dietschy. 1971. Unstirred water layers in intestine: rate determinant of fatty acid absorption from micellar solutions. *Science (Wash. D. C.)* 174: 1031-1033.
15. Lukie, B. E., H. Westergaard, and J. M. Dietschy. 1974. Validation of a chamber that allows measurement of both tissue uptake rates and unstirred layer thickness in the intestine. *Gastroenterology*. In press.
16. Gregg, J. A. 1966. New solvent systems for thin-layer chromatography of bile acids. *J. Lipid Res.* 7: 579-581.
17. Eneroth, P. 1963. Thin-layer chromatography of bile acids. *J. Lipid Res.* 4: 11-16.
18. Hofmann, A.F. 1962. Thin-layer adsorption chromatog-

- raphy of free and conjugated bile acids and silicic acid. *J. Lipid Res.* 3: 127-129.
19. Diamond, J. M. 1966. A rapid method for determining voltage-concentration relations across membranes. *J. Physiol.* 183: 83-100.
  20. Sallee, V. L., F. A. Wilson, and J. M. Dietschy. 1972. Determination of unidirectional uptake rates for lipids across the intestinal brush border. *J. Lipid Res.* 13: 184-192.
  21. Fisher, R. B., and D. S. Parsons. 1950. The gradient of mucosal surface area in the small intestine of the rat. *J. Anat.* 84: 272-282.
  22. Palay, S. L., and L. J. Karlin. 1959. An electron microscopic study of the intestinal villus. II. The pathway of fat absorption. *J. Biophys. Biochem. Cytol.* 5: 373-383.
  23. Holz, R., and A. Finkelstein. 1970. The water and nonelectrolyte permeability induced in thin lipid membranes by the polyene antibiotics nystatin and amphotericin B. *J. Gen. Physiol.* 56: 125-145.
  24. Sherrill, B. C., J. G. Albright, and J. M. Dietschy. 1973. Diffusion studies of bile acids, fatty acids and sucrose-NaCl-water systems at 37°C by a modified capillary cell apparatus and their application to membrane transport studies. *Biochim. Biophys. Acta.* 311: 261-271.
  25. Diamond, J. M., and E. M. Wright. 1969. Biological membranes: the physical basis of ion and nonelectrolyte selectivity. *Annu. Rev. Physiol.* 31: 581-646.
  26. Diamond, J. M., and E. M. Wright. 1969. Molecular forces governing nonelectrolyte permeation through cell membranes. *Proc. R. Soc. Lond. B. Biol. Sci.* 172: 273-316.
  27. Wright, E. M., and J. M. Diamond. 1969. Patterns of non-electrolyte permeability. *Proc. Roy. Soc. Lond. B. Biol. Sci.* 172: 227-271.
  28. Wright, E. M., and J. W. Prather. 1970. The permeability of the frog choroid plexus to nonelectrolytes. *J. Membr. Biol.* 2: 127-149.
  29. Hingson, D. J., and J. M. Diamond. 1972. Comparison of nonelectrolyte permeability patterns in several epithelia. *J. Membr. Biol.* 10: 93-135.
  30. Frömter, E., and J. Diamond. 1972. Route of passive ion permeation in epithelia. *Nat. New Biol.* 235: 9-13.
  31. Sallee, V. L., J. M. Dietschy, and F. C. Rector, Jr. 1972. Monomer diffusion as the mechanism of intestinal fatty acid uptake from bile acid micelles. *Fed. Proc.* 31: 259. (Abstr.)
  32. Winne, D. 1973. Unstirred layer, source of biased Michaelis constant in membrane transport. *Biochim. Biophys. Acta.* 298: 27-31.